

# Effects of Surface Topography on the Connective Tissue Attachment to Subcutaneous Implants

Hugh Kim, DMD, MSc<sup>1</sup>/Hiroshi Murakami, DDS, PhD<sup>2</sup>/Babak Chehroudi, DMD, PhD<sup>1</sup>/  
Marcus Textor, PhD<sup>3</sup>/Donald M. Brunette, PhD<sup>4</sup>

**Purpose:** A major concern for implants that penetrate stratified epithelia is aggressive epithelial proliferation and migration. This epithelial downgrowth on the implant can be inhibited by a firm attachment between the underlying connective tissue and the implant. This study evaluates the connective tissue attachment to titanium implants with various well-defined surface topographies. **Materials and Methods:** Titanium-coated epoxy replicas of polished (PO;  $R_a = 0.06 \mu\text{m}$ ), finely blasted (FB;  $R_a = 1.36 \mu\text{m}$ ), coarsely blasted (CB;  $R_a = 5.09 \mu\text{m}$ ), acid-etched (AE;  $R_a = 0.59 \mu\text{m}$ ), coarsely blasted and acid-etched (SLA;  $R_a = 4.39 \mu\text{m}$ ), titanium plasma-sprayed (TPS;  $R_a = 5.85 \mu\text{m}$ ), machined-like (ML;  $R_a = 2.15 \mu\text{m}$ ), and micromachined grooved (GR; V-shaped grooves 30  $\mu\text{m}$  deep) surfaces were implanted subcutaneously in 74 rats for 1 to 11 weeks. Animals were sacrificed weekly. Surfaces were processed for histomorphometric evaluation of connective tissue attachment, capsule thickness, and where applicable, the degree of separation between the tissue and implant. **Results:** A total of 153 test surfaces were analyzed. Statistical analysis revealed that textured and rough substrata, namely the GR, TPS, AE, CB, and SLA surfaces, exhibited significantly greater ( $P < .05$ ) connective tissue attachment and thinner fibrous encapsulation when compared to the PO surface. Tissue separation from the implant interface was of significantly lower magnitude and frequency with the rough surfaces than with the PO surface. **Conclusions:** The results indicate that rough implant surfaces are associated with stable connective tissue attachment, which has implications for their use in percutaneous and permucosal applications. In addition, data from the AE surface may indicate that the geometry of the surface irregularities can also be a significant determinant of the connective tissue response. (Basic Science) (More than 50 references) INT J ORAL MAXILLOFAC IMPLANTS 2006;21:354–365

**Key words:** connective tissue attachment, fibrous capsule, surface topography, tissue-implant interface

Research on the titanium implant-tissue interface generally concentrates on the integration of the alloplast with bone.<sup>1–4</sup> The in vivo soft tissue

response to titanium has received comparatively less attention, despite the need for an endosseous implant to pass through connective tissue and epithelium when supporting a dental prosthesis. Epithelium fulfills an important role in implant function by sealing percutaneous and dental implants from contaminants in the external environment.<sup>5</sup> However, epithelium's tendency to proliferate and migrate along an implanted device can create sinus tracts that may undermine the implant and lead to its loss.<sup>6–12</sup> Aggressive epithelial downgrowth can be impeded by a firm attachment between the soft connective tissue and the implant, with cells and fibers attached to the implant surface, as is the case with Sharpey's fibers around natural teeth.<sup>6</sup> In healthy tissue, collagen bundles insert into the root cementum; the connection deters downward migration of the overlying epithelium.<sup>13</sup> Connective tissue does not usually attach to titanium substrata in this man-

<sup>1</sup>Assistant Professor, Department of Oral Biological and Medical Sciences, Faculty of Dentistry, University of British Columbia, Vancouver, British Columbia, Canada.

<sup>2</sup>Assistant Professor, Fixed Prosthodontics, School of Dentistry, Aichi-Gakuin University, Nagoya, Japan.

<sup>3</sup>Professor, Laboratory for Surface Science and Technology, Department of Materials, Swiss Federal Institute of Technology, Zurich, Switzerland.

<sup>4</sup>Professor and Acting Head, Department of Oral Biological and Medical Sciences, and Associate Dean (Research), Faculty of Dentistry, University of British Columbia, Vancouver, British Columbia, Canada.

**Correspondence to:** Dr Donald M. Brunette, Faculty of Dentistry, University of British Columbia, 360-2199 Wesbrook Mall, Vancouver, BC V6T 1Z3. Fax: +604 822 3562. E-mail: brunette@interchange.ubc.ca

ner.<sup>14,15</sup> Instead, connective tissue typically becomes organized into a fibrous capsule, with collagen fibers oriented parallel to the implant surface.<sup>6,8,11,12,15,16</sup> The presence of this fibrous capsule often denotes a failure of the implant to integrate with the soft tissues. In addition to compromising local blood supply, thick fibrous capsules are associated with a persistent fluid space between the tissue and the implant, precluding stable implant fixation.<sup>17</sup>

A promising approach to optimizing soft tissue-implant integration involves modification of the topography of the implant surface. The surface topography of implanted biomaterials is known to modulate host response at the cellular level. For example, Keller and associates demonstrated that titanium surfaces roughened by blasting and/or acid etching are more conducive to osteoblast attachment than smooth surfaces.<sup>18</sup> Their *in vitro* data further supports the use of roughened implant surfaces to enhance bone integration *in vivo*.<sup>3,4,18</sup> It is also conceivable that the ideal implant surface would optimize connective tissue attachment with appropriate orientation while minimizing fibrous capsule formation. The effects of surface topography on fibroblast attachment have been documented both *in vitro*<sup>19–24</sup> and *in vivo*.<sup>6,17,25–27</sup> It was thus hypothesized that roughened implant surface topographies designed to improve bone integration would be effective for soft tissue integration as well.

The aim of the present *in vivo* study was to evaluate the soft tissue response to various implant surface topographies subcutaneously in a rat model using the histomorphometric parameters of attachment, capsule thickness, and degree of tissue-implant separation. The subcutaneous model was chosen for its simplicity, since it allowed the study of connective tissue behavior without the complications of epithelial downgrowth or biofilm formation.

## MATERIALS AND METHODS

Seven of the 8 surface topographies used in this investigation were replicated using disks (15 mm diameter, 1 mm width) of grade 2 commercially pure titanium. The surface topographies were provided by Institut Straumann (Basel, Switzerland) and were defined and manufactured as follows:

1. Machined-like (ML): The term *machining* refers to the lathing, milling, or cutting of metal objects. A machined surface topography is characterized by fine parallel grooves oriented in the direction of cutting.<sup>28</sup> In this study, the titanium disks were treated with 60-grit silicon carbide (SiC) grinding paper to produce a striated surface resembling a machined surface.
2. Polished (PO): The titanium disks were treated with 60-grit SiC grinding paper, then polished to a mirror finish with a 10- $\mu\text{m}$  diamond paste in oil and a 0.06- $\mu\text{m}$  silicon dioxide (SiO<sub>2</sub>) suspension.
3. Finely blasted (FB): The titanium surface was blasted with glass beads 150 to 230  $\mu\text{m}$  in diameter.
4. Coarsely blasted (CB): The titanium surface was blasted with alumina particles 200 to 500  $\mu\text{m}$  in diameter.
5. Acid-etched (AE): The titanium surface was treated in a hot solution of hydrochloric acid (HCl) and sulfuric acid (H<sub>2</sub>SO<sub>4</sub>).
6. Sandblasted, large-grit, acid-etched (SLA): This surface was obtained by blasting the titanium surface with 250- $\mu\text{m}$ -diameter alumina particles prior to etching with HCl/H<sub>2</sub>SO<sub>4</sub>.
7. Titanium plasma-sprayed (TPS) surface: This surface was obtained by blasting the titanium surface with 250- $\mu\text{m}$ -diameter alumina particles and plasma-spraying the surface with titanium hydride powder.
8. Micromachined silicon surface (GR): The eighth surface was produced by etching parallel grooves onto silicon substrata using a technique first described by Camporese and colleagues.<sup>29</sup> In brief, following protection of the silicon substrata with a layer of silicon dioxide and a photosensitive agent, the surface is exposed to intense light through a computer-generated photomask. The light dissolves the photosensitive coating at the planned groove sites, selectively exposing the underlying silicon dioxide-coated silicon substrata. Next, the exposed portions of the SiO<sub>2</sub> coating are chemically dissolved, in turn selectively exposing the silicon according to the desired pattern. Finally, the silicon surface is anisotropically etched to form V-shaped grooves.<sup>30</sup> The grooves on the disks used in this study were 30  $\mu\text{m}$  deep and 35  $\mu\text{m}$  wide, with a pitch of either 40 or 45  $\mu\text{m}$  (Fig 1).

The roughness of the surfaces was quantified by noncontact laser profilometry. For each surface, 7 profiles were randomly obtained over a measurement distance of 4.096 mm. The lateral resolution of this technique was 1  $\mu\text{m}$ .<sup>31</sup> This technique was used to determine the  $R_a$  value for each surface, which is defined as the average height deviation, or amplitude, of the surface irregularities (Table 1). Although  $R_a$  values were of the greatest interest, the surface topographies were also characterized by other numerical parameters, including  $R_q$ ,  $R_t$ ,  $R_{zDIN}$ ,  $S_m$ ,  $S_k$ , and  $L_z$ . These additional parameters have been defined and outlined by Wieland and coworkers.<sup>31,32</sup>

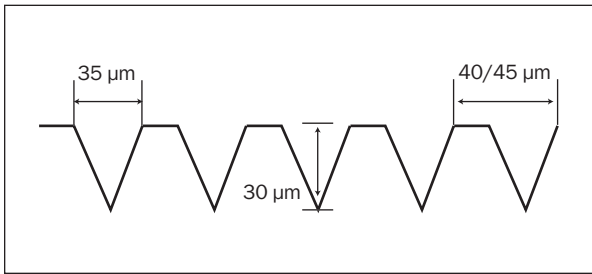


**Fig 1** Schematic representation of the micromachined grooved surface. The V-shaped grooves were 30 μm deep and 35 μm wide, with a pitch of either 40 μm or 45 μm.

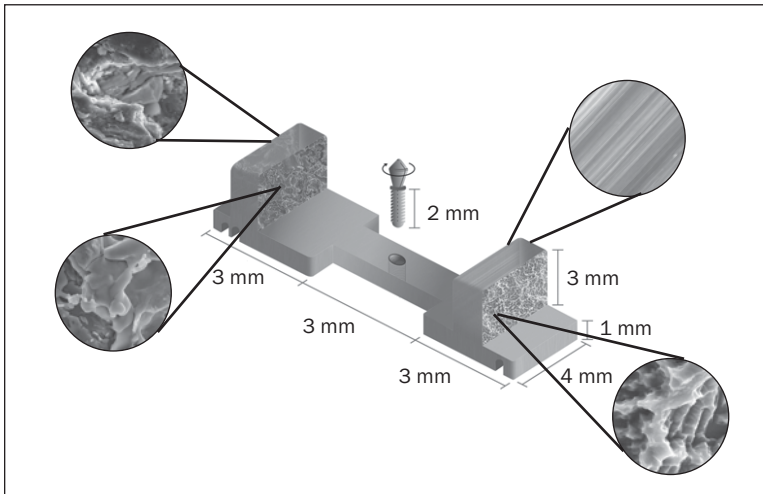


**Fig 2** Schematic representation of the implant. There were 4 test surfaces per implant. The test surfaces were located on the sides of the vertical components (posts).

**Table 1** Effect of Surface Type on Suitability for Morphometric Analysis and Incidence of Complete Attachment/Detachment

Surface type	R <sub>a</sub> value	No. of surfaces processed	Surfaces suitable*		Surfaces with complete attachment† (%)	Surfaces with partial attachment† (%)	Surfaces with complete detachment† (%)
			n	%			
PO	0.06	38	16	42	0	69	31
FB	1.36	19	6	32	0	17	83
ML	2.15	55	26	47	8	73	19
AE	0.59	55	28	51	21	54	25
GR	N/A	71	38	54	10	77	13
SLA	4.39	19	16	84	18	82	0
CB	5.09	19	10	53	50	50	0
TPS	5.85	19	13	68	38	62	0

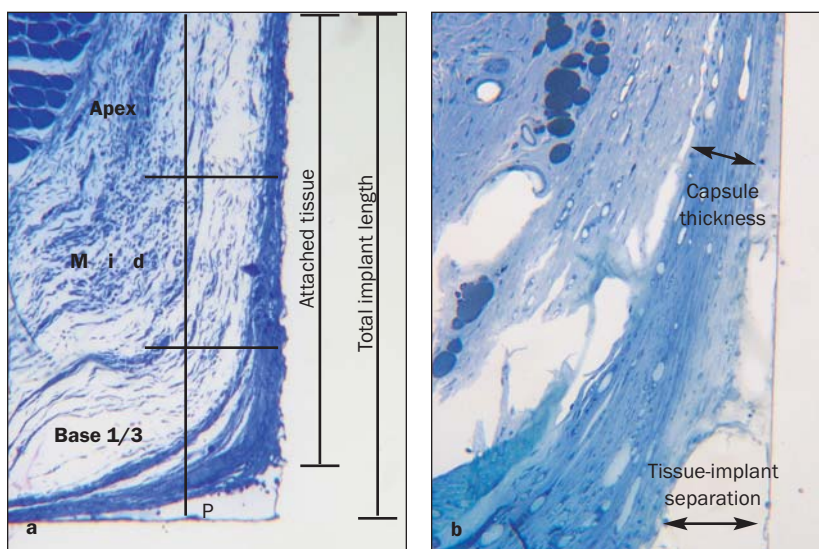
\*Number/percentage of processed surfaces that were suitable for morphometric analysis.

†Complete attachment refers to surfaces with tissue attachment along the entire implant length; partial attachment refers to surfaces with tissue attachment along part of the implant length; complete detachment refers to surfaces devoid of any tissue attachment.

All topographies were replicated onto epoxy resin to form exact duplicates of the original surfaces. This method of replication has been shown to accurately reproduce the original surface textures.<sup>6,31</sup> In brief, impressions were made of the titanium and silicon surfaces using Pro-Vilnovo polyvinyl siloxane impression material (Heraeus Kulzer, Hanau, Germany). Epoxy resin (EPO-TEK 302-3; Epoxy Technology, Bellerica, MA) was then poured into the impressions to obtain the replicas. Replicas were cleaned with 7×

detergent (ICN Biomedicals, Aurora, OH) and washed with distilled water 20 times. After 30 minutes of ultrasonication, replicas were sputter-coated with 50 nm of titanium using the Randex 3140 Sputtering System (Palo Alto, CA). The surfaces were subsequently sterilized by glow-discharging for 3 minutes in an argon gas chamber, fabricated according to the design of Aebi and Pollard.<sup>33</sup> From the epoxy replicas, U-shaped devices were fabricated for subcutaneous implantation. Each implant consisted of 2 ver-

**Fig 3** Schematic representation of the morphometric parameters. (a) The attached tissue was assessed as a percentage of the total implant length. Note the 90-degree angle between the test surface and the implant pedestal (P). The implant was divided into 3 zones for study at higher magnification. (b) View of a single implant zone. The thickness of the fibrous capsule was measured 5 times per zone (15 times per implant), as was the distance between tissue and implant in areas of separation (toluidine blue; original magnification  $\times 32$  [left] and  $\times 100$  [right]).



tical posts connected at their base by a pedestal.<sup>6,34</sup> Each post had 2 opposing titanium-coated implant surfaces. Therefore, a single implant exhibited 4 test surfaces (Fig 2).

X-ray photoelectron spectroscopy was used to analyze the surface chemical composition of the titanium-coated replicas. This assay determined the proportions of elemental titanium, oxygen, carbon, and nitrogen (atom %). The data indicated that the chemical composition was the same for all surfaces regardless of topography.<sup>31</sup>

The surgical procedure used in this study has been described previously.<sup>35</sup> A total of 74 implants were placed subcutaneously in the parietal area in male Sprague-Dawley rats. The test surfaces of the implant were in the soft tissue, while the pedestal of the implant was secured to the underlying bone with a miniature titanium screw (Fig 2). Animals were sacrificed at weekly intervals up until 11 weeks postimplantation. Between weeks 1 and 10, 7 animals were sacrificed per week (28 surfaces processed weekly). During week 11, 4 animals were sacrificed (16 surfaces processed). After the tissue was perfused with 2.5% glutaraldehyde, the implants were removed together with the parietal bone and placed in Karnovsky's fixative for 24 hours at 4°C, followed by 2% buffered osmium tetroxide for 4 hours. The specimens were dehydrated in a graded water-miscible resin (Aquembed; Ladd Research Industries, Burlington, VT), infiltrated with graded Aquembed/ Epon, and finally embedded in Epon (JB EM, Dorval, Québec, Canada).

Using a Sorvall MT2 microtome (Thermo Electron/Sorvall, Waltham, MA), 2- $\mu$ m-thick sections were cut parallel to the long axis of the implant, stained

with 1% toluidine blue, and examined under a light microscope. Photomicrographs were taken using a Canon EOS D60 digital camera (Canon, Tokyo, Japan). Measurements were made using National Institutes of Health Image 1.63 software (NIH, Bethesda, MD).

Low-magnification photographs (32 $\times$ ) were made of the entire implant length. The length of the implant surface and the area of the attached tissue were measured. The attachment was expressed as a percentage of the total implant length (Fig 3a) using the following formula: % attachment = (length of attached tissue  $\div$  total implant length)  $\times$  100.

To measure capsule thickness and tissue-implant separation, the entire length of the implant was divided into 3 zones, each representing one third of the implant length: (1) the base (pedestal) of the implant, (2) the middle third of the implant, and (3) the apex (area closest to the skin). For each zone, a photomicrograph was obtained at a higher magnification (100 $\times$ ) in order to measure capsule thickness and tissue-implant separation (Fig 3a). In each zone, the thickness of the fibrous capsule was measured at 5 points along the implant length, 200  $\mu$ m apart. Capsule thickness was therefore measured in 15 places per section. In areas of tissue detachment from the implant surface, measurements of the distance between tissue and implant were performed and repeated in the same manner as for capsule thickness (Fig 3b).

A multivariate analysis of variance (MANOVA) and Bonferroni post-hoc multiple comparison tests were used to assess the parameters of percent tissue attachment, capsule thickness, and degree of tissue-implant separation as functions of surface type and time. The data were grouped into 2 time periods: (1)

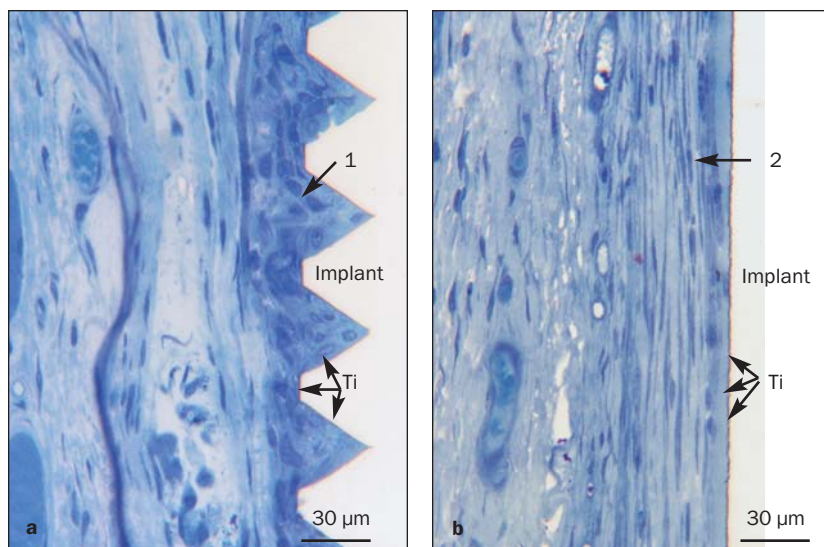


**Fig 4** Photomicrographs of the (a) GR and (b) ML implant surfaces. Note the oblique orientation of the fibroblasts onto the grooved surface (arrow 1). Fibroblasts were organized into a fibrous capsule parallel to the machined surface (arrow 2). Ti = titanium coating (toluidine blue).

the early healing stage (weeks 1 through 5) and (2) the late healing stage (weeks 6 through 11). These time periods were chosen based on past studies comparing the early and late stages of implant healing. It has been demonstrated that the sixth week represents the time at which the peri-implant fluid space disappears and the cells contact the implant surface directly.<sup>15,36,37</sup> Data were obtained throughout each period to cover a wide range of events within each period. The null hypothesis was rejected at  $P < .05$ .

## RESULTS

A wide range of surface roughnesses and configurations was selected for this study to represent the common commercially available implant surfaces. The use of epoxy replicas allowed histologic sectioning of the tissue-implant interface in toto. The replication process faithfully reproduced the topographies and details of the original surfaces. Details regarding technique and surface specifications are explained in 2 previous publications.<sup>31,32</sup>

A number of uncontrollable factors affected the outcome of the in vivo implantation procedures. For example, infection and hematoma formation were noted with a number of the implants, which rendered the processed tissue unsuitable for histologic analysis. This complication resulted in reduced sample sizes of certain test surfaces. Table 1 shows the number of samples of each test surface found suitable for analysis.

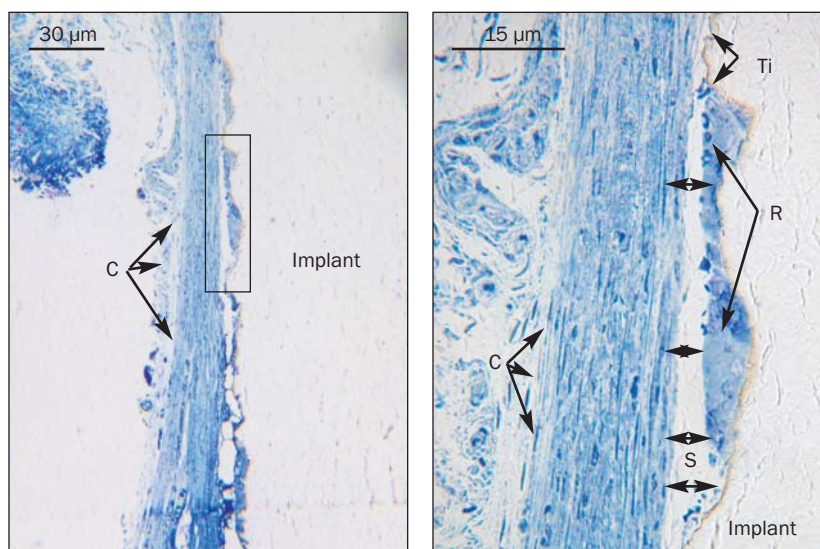
Another major challenge involved obtaining histologic sections from the implant-tissue interface. The different hardness values of the embedding resin, epoxy implant, and titanium coating resulted in

wrinkles, tissue separation, and scratch marks on many sections, making them unusable for histomorphometric analysis. These problems were addressed by adjusting the speed of the sectioning and the angle of the glass knife. Nevertheless, numerous histologic samples had to be discarded on account of such artifacts. Another difficulty that arose was the presence of thick capsules, which were often associated with large, thick tissue samples and which frequently prevented adequate resin infiltration. Excessive volumes of tissue were meticulously trimmed under a dissecting microscope prior to embedding. Some samples were also re-embedded.

A great number of the samples showed connective tissue in contact with the surface along part of the implant length. The healing pattern appeared to be similar for all surfaces. Early healing was characterized by the accumulation of fibrin-rich tissue seeded with undifferentiated mesenchymal cells, neutrophils, lymphocytes, and monocytes. By the first week of healing, elongated fibroblasts appeared near the implant surface, along with numerous blood vessels. On the GR surface, fibroblasts were often observed in the grooves (Fig 4a). On all the other substrata, fibroblasts were typically elongated parallel to the implant surface and organized into a multilayered fibrous capsule (Fig 4b). The thickness of the capsule appeared to decrease with time on most surfaces. The AE, GR, SLA, CB, and TPS surfaces had thinner capsules whose dimensions did not change appreciably during the study period.

Areas of tissue separation from the implant surface were consistently observed, often where the implant body connected to the base at a 90-degree angle (Fig 3a). It could not be determined whether the detachment occurred in situ or during histologic

**Fig 5** Area of tissue detachment (S) from a coarsely blasted implant. Note the residual tissue (R) on the implant surface. Ti = titanium coating, C = capsule (toluidine blue).



processing. In either case, detachment of tissue from the implant surface indicated weak tissue attachment. For the SLA, TPS, GR, and CB surfaces, some remaining cells could be seen on the implant surfaces even in areas of tissue detachment (Fig 5). Residual tissue was not observed for any of the other 4 test surfaces.

The histomorphometric analysis was based on a total of 6,120 measurements collected from 153 samples representing the 8 test surfaces. Data from the FB surface were excluded from consideration, since only 1 suitable sample was obtained during the early healing period, although 5 samples were obtained during the late healing period. MANOVA revealed that both surface type and time had a statistically significant effect on each of the 3 dependent variables: (1) attachment, (2) capsule thickness, and (3) the lateral distance separating tissue and implant in areas of separation.

Attachment was determined as the percentage of the implant length in contact with the contiguous soft tissue. The substrata with the higher  $R_a$  values, namely the TPS, CB, SLA, and GR surfaces, demonstrated the highest levels of attachment during both time periods, representing a statistically significant difference ( $P < .05$ ) when compared to the smoother ML and PO surfaces (Table 2). By the later stage of healing (weeks 6 to 11), the mean attachment on the 3 roughest test surfaces (CB, SLA, TPS) was approximately 4 times that of the PO surface. Comparisons between time periods show that attachment remained constant on the PO, CB, and GR surfaces, while increasing on the ML, AE, SLA, and TPS surfaces. The ML surface showed a 3-fold increase in mean attachment levels between the 2 time periods. Although not included in the statistical analysis, the

FB surface exhibited the least attachment among all test surfaces during both time periods.

Complete tissue attachment was deemed to have occurred when tissue contacted the implant along its entire length, with no areas of separation (Figures 6a to 6c). The CB and TPS surfaces showed the highest incidence of complete attachment (50% and 38% of samples, respectively; Table 1). Complete attachment was not observed on any of the PO or FB samples and was seen on only 8% of the ML samples. Conversely, complete detachment refers to an implant surface that was completely devoid of tissue contact (Fig 6d). Complete detachment was observed on 83% of the FB surfaces and on 31% of the PO surfaces. Complete detachment was not observed on any of the SLA, TPS, or CB samples.

The fibrous capsule was delineated from the surrounding tissue based on differences in cell orientation. In addition, the toluidine blue stained the fibrous capsule more intensely than the peripheral tissue. For both time periods, the thickest capsules were found around the PO, FB, and ML surfaces. There was a statistically significant difference ( $P < .05$ ) when the mean capsule thickness of the PO surface was compared to that of the other test surfaces (Table 2). For example, during the early healing stage (weeks 1 to 5), the PO and FB surfaces harbored capsules that were approximately twice as thick (122 to 144  $\mu\text{m}$ ) as those around the AE, GR, SLA, TPS, and CB surfaces (50 to 64  $\mu\text{m}$ ), while the ML surface presented an intermediate capsule thickness (76  $\mu\text{m}$ ). The effect of time on capsule width varied between surface types. The capsule thickness of the PO surface during the second healing period (75  $\mu\text{m}$ ) was significantly less ( $P < .05$ ) than its thickness during the first healing period (123  $\mu\text{m}$ ), approximately half

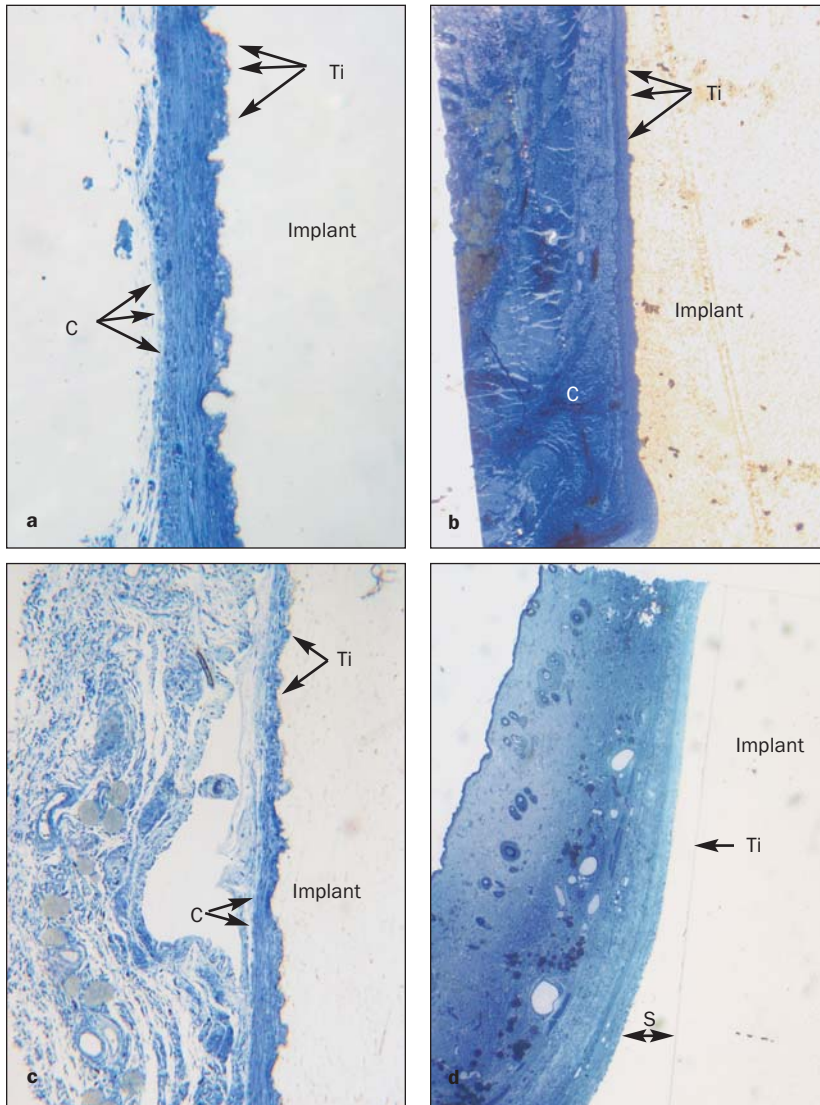


**Fig 6** Photomicrographs of (a) TPS, (b) SLA, and (c) CB implants showing complete tissue attachment along the implant lengths. Note the complete absence of tissue attachment adjacent to (d) the PO implant. S = separation, Ti = titanium coating, C = capsule.

**Table 2** Effect of Surface Type and Healing Stage on Attachment, Capsule Thickness, and Tissue-Implant Separation

Surface type	Surfaces (n)		Mean tissue attachment <sup>‡</sup>		Mean capsule thickness (µm)		Mean tissue separation (µm)	
	Early	Late	Early	Late	Early	Late	Early	Late
PO	9	7	22.46 ± 10.35	22.28 ± 6.94	122.55 ± 19.1	75 ± 22.04	213.94 ± 70.03	57.25 ± 18.15
FB <sup>†</sup>	1	5	0*	8.88 ± 8.88	144*	114.65 ± 11.92	252.76*	104.29 ± 28.82
ML	13	13	18.71 ± 7.67	60.88 ± 9.57	76.03 ± 8.38	90.46 ± 11.22	71.12 ± 19.16	50.46 ± 20.5
AE	14	14	43.66 ± 13.04	65.24 ± 10.19	50.81 ± 7.83	50.94 ± 4.31	44.62 ± 15.7	41.26 ± 12.89
GR	16	22	62.55 ± 7.96	58.02 ± 7.93	62.04 ± 6.99	62.96 ± 5.6	50.14 ± 13.6	66.45 ± 20.48
SLA	8	8	70.49 ± 6.84	90.44 ± 7.93	64.19 ± 8.69	54.7 ± 7.97	43.2 ± 14.57	20.52 ± 11.17
CB	4	6	100 ± 0	98.51 ± 1.49	64.12 ± 26.05	52.58 ± 4.8	29.26 ± 21.7	0.89 ± 0.88
TPS	6	7	75.48 ± 15.35	94.80 ± 2.67	59.37 ± 11.1	64.39 ± 9.23	27.31 ± 11.34	18.88 ± 9.36

\*Only 1 sample was available for the FB surface at this time period.

<sup>†</sup>Surface was excluded from statistical analysis.

<sup>‡</sup>Attachment was determined as the percentage of the implant length in contact with the contiguous soft tissue.

the size. Decreases in capsule thickness for the SLA and CB surfaces were not statistically significant ( $P > .05$ ). No other surface type exhibited a time-related decrease in capsule thickness.

The PO surface demonstrated tissue separation from the implant surface that was 5 to 10 times greater when compared to the TPS, SLA, CB, and AE surfaces (Table 2). This difference was statistically significant ( $P < .05$ ). The data showed a general trend toward decreasing separation from 1 time period to the next, implying that the tissue approached the implant surface over time. The most striking observation in this regard was with the PO surface, where the tissue-implant distance underwent a decrease between the 2 time periods from 214  $\mu\text{m}$  to 57  $\mu\text{m}$ .

The PO and FB surfaces ranked among the smoothest test surfaces and demonstrated the greatest capsule thickness, the least amount of attachment, and the greatest degree of tissue-implant separation. In contrast, the rougher SLA, TPS, and CB surfaces displayed significantly ( $P < .05$ ) thinner capsules, greater attachment, and less tissue-implant separation.

## DISCUSSION

The topographical features of an implant surface are known to affect soft tissue response *in vivo*.<sup>6,17,25</sup> A number of *in vivo* studies have employed polymeric implants,<sup>27,38,39</sup> whereas fewer studies have examined the soft tissue reaction to roughened titanium substrata.<sup>15</sup> Most studies of rough titanium surfaces have investigated their effects on bone integration.<sup>3,4,40–43</sup> The aim of the present investigation was to examine, in a subcutaneous rat model, the *in vivo* soft tissue attachment to surface topographies of varying roughness, including titanium-coated replicas of commercially available dental implant surfaces. The implant-soft tissue interface was assessed histologically and quantitatively using the morphometric parameters of attachment, fibrous capsule thickness, and where applicable, the degree of tissue separation from the implant surface.

The smoothest substrata used in this investigation demonstrated the thickest fibrous capsule formation, the least amount of attachment, and the greatest degree of tissue-implant separation. In contrast, the roughest surfaces displayed significantly thinner fibrous capsules, greater connective tissue attachment, and the least tissue-implant separation. The ML surface, representing an intermediate degree of roughness, presented capsule thickness, attachment, and separation values that were approximately mid-way between the smoothest and roughest surfaces.

An exception to this general rule was the AE surface. It had the second-lowest  $R_a$  value among the test surfaces, yet its capsule thickness and separation data were comparable to those of the SLA, TPS, and CB surfaces. Acid etching is a widely-used method for implant surface treatment that has been used alone or in conjunction with other methods such as blasting.<sup>4,44</sup> The current study indicated that the etched surface, despite its low roughness value, promoted connective tissue integration comparable to that of much rougher surfaces. It is possible that the unique geometry created by the etching procedure can play a dominant role in promoting connective tissue integration.

Fibroblasts and the extracellular matrix tend to interdigitate into the rough surfaces and secure the implant in position.<sup>45,46</sup> Such an implant would be expected to be mechanically stable and resistant to dislodgment forces. In contrast, smoother surfaces tend to promote a thick, nonintegrated fibrous capsule, which is less likely to support and secure the implant in its location.<sup>47</sup> A more secure implant will reduce the micromotion at the interface, which could indirectly promote healing with a thinner capsule. These findings are in agreement with those of Ungersböck and associates,<sup>17</sup> who cited mechanical stability and intimate tissue adhesion as the causes for thinner fibrous capsules around blasted ( $R_a = 1.50$ ) as compared to polished ( $R_a = 0.19$ ) titanium implants after a 3-month implantation period in rabbits.

Schroeder and colleagues<sup>25</sup> reported on collagen fibers inserted perpendicularly into rough titanium-sprayed implant surfaces placed in primates. In the study by Schroeder and colleagues, the application of tensile stress at the implant interface tore out particles of the rough surface, suggesting firm tissue anchorage. In the present study, evidence of firm attachment was often present on the SLA, CB, and TPS surfaces where either no tissue detachment was noted or detachment occurred within the tissue and not at the implant surface. The lack of detachment indicates a strong connective tissue adhesion with the rough surfaces. Chou and colleagues<sup>48</sup> reported that cell shape, in particular cell height or thickness, is affected by the surface topography of the substratum and promotes the expression of the adhesion protein fibronectin. Similarly, Wieland and coworkers<sup>31</sup> found that fibroblasts cultured on the CB, TPS, and SLA surfaces had a greater thickness than cells cultured on smoother surfaces. The preferential expression and adsorption of fibronectin to the rough surfaces along with mechanical interlocking could provide a partial explanation for the greater attachment found with the SLA, TPS, and CB implants.



The ML, AE, SLA, and TPS surfaces showed a statistically significant increase in the attachment between the early and late stages of healing. The time-related increase in attachment was not observed for the PO surface, implying that connective tissue attachment to the rough surfaces continues to improve during the late stage of healing. It is possible that following early tissue detachment, the rough implant surfaces became repopulated, with new tissues originating from cells remaining on the implant surface.

The residual tissue found on rough surfaces in areas of separation may represent detachment that occurred during histologic processing rather than *in situ*. The absence of residual tissue on smooth implants suggests that the implants never fostered attachment. In any event, data from the present study indicate that the greatest degree of tissue separation from the implant surface occurred at the PO, FB, and ML implants. One explanation for this observation could relate to the tendency of the fibrous capsule to contract, leading to tissue separation away from the implant surface. Capsular contracture around implants is a major complication in reconstructive and esthetic breast surgery. There is abundant literature focused on the effect of breast implant texturing on capsule formation and contraction. Several studies indicate that textured breast implants are associated with less capsule contraction than implants with smooth, polished surfaces.<sup>45,49-53</sup> Histologic observations around smooth breast implants have shown that fibroblasts and collagen fibers align parallel with the implant surface, whereas textured implants foster a multidirectional collagen fiber orientation.<sup>52</sup> These histologic findings are supported by the current observations of oblique fibroblast orientation on surfaces with 30- $\mu\text{m}$  grooves and the parallel arrangement seen on the PO surface. A multidirectional collagen organization directs contractile forces in different paths, resulting in the neutralization or reduction of the magnitude of forces that cause tissue separation.<sup>49</sup> Rubino and colleagues<sup>53</sup> also reported that the capsule tissue immediately adjacent to textured breast implants had a random collagen fiber orientation and was noncontractile. In contrast, the outer capsule layers not affected by the surface texture were composed of fibers with a parallel orientation. Rubino and colleagues speculated that this is the only layer where contractile forces could be generated by the capsule. The increased capsular contraction observed around smooth silicone implants is consistent with the observations of smooth titanium-coated implants in the current study. It can thus be inferred that the thicker capsules of parallel collagen fibers formed around PO and FB implants create a greater contractile force than that generated by the capsules

around the rougher surfaces. The contractile force is likely generated by myofibroblasts within the parallel-oriented fibers.<sup>54-56</sup> In the current study, the capsule was typically attached at 2 locations: on the test surface and on the pedestal. The alignment and contraction of the collagen fibers between these 2 points would retract the tissue away from the implant surface, analogous to the straightening of a bow upon release of the arrow. The greater tissue-implant separation observed with the smoother surfaces is also suggestive of a weak attachment, although detailed quantitative assessments of tissue attachment strength would be required to directly substantiate this hypothesis.

The CB, TPS, and SLA surfaces promoted the greatest connective tissue attachment. This attachment improved significantly with time, an observation that bodes well for their clinical performance in perimucosal or percutaneous applications. For example, while great emphasis has been placed on the integration of dental implants into bone, the integration of the overlying soft tissue around transmucosal components has been studied less extensively *in vivo*.<sup>15</sup> The dental implant is anchored in bone and connected to the prosthetic tooth via an abutment that projects through the mucosa. The transmucosal abutment links the bone-integrated fixture to the prosthetic tooth. The abutment surface should thus be conducive to a firm soft tissue seal between the implant and the harsh oral environment. The most commonly used implant abutments have either a machined or polished surface.<sup>57,58</sup> The mucosal response around implant abutments with differing surface topographies in dogs<sup>16,59</sup> and in humans<sup>60</sup> has been examined in recent studies. Machined, blasted, and acid-etched surface topographies were compared; no significant differences were found in the length of the connective tissue attachment to the abutments. However, the surfaces used in these studies did not possess average height deviations greater than 1.87  $\mu\text{m}$ , which is in contrast to the height deviations of the rougher surfaces used in the present study (4.39 to 5.85  $\mu\text{m}$ ). Since the roughness characterization techniques used in the current study were similar to those used by Wennerberg and associates,<sup>60</sup> it can be inferred that considerably rougher surfaces were used in the current study. It is possible that the greater surface roughness allowed for superior tissue interlocking and a more substantive connective tissue attachment. In spite of this, it appears that the geometry of the surface irregularities can be as important as their size, since the AE surface in the present study presented capsule thickness and separation data comparable to those of much rougher surfaces.

The present study suggests that roughened surfaces can improve the connective tissue attachment to the transmucosal portions of dental implants. However, it should be noted that epithelial cell attachment and proliferation are markedly reduced on rough titanium.<sup>61,62</sup> It should also be noted that rough surfaces exposed to the oral cavity have a propensity to accumulate dental plaque.<sup>63</sup> Although canine biopsies of implants obtained by Zitzmann and associates<sup>59</sup> showed no difference in the size or composition of the plaque-induced inflammatory lesion, the potential for plaque accumulation can nonetheless be addressed by a differential texturing of the abutment. Specifically, the abutment could have a TPS or SLA-like surface in its lower portion to maximize fibroblast adhesion and promote a stable connective tissue seal, whereas its upper portion, the portion closest to the oral cavity, could feature a smoother surface to favor epithelial adhesion while minimizing plaque retention.

The implant design used in this study had a 90-degree angle between the test surface and the pedestal (base). The abrupt boundary between the test surface and the pedestal had the potential to hinder a stable contact between tissue and implant, creating a dead space at the base. Sanders and Rochefort<sup>64</sup> placed polymer fiber implants subcutaneously at varying angles to the skin. Their study concluded that the likelihood of fibrous capsule formation was dependent on the degree to which the implant was placed parallel to the skin surface. According to Sanders and Rochefort, fibrous encapsulation was avoided when implants were placed parallel to the skin surface. When the implant was placed at an angle relative to the skin surface, a dead space was created, attracting inflammatory cells and leading to the formation of a fibrous capsule. The observations of Sanders and Rochefort are consistent with the lack of attachment and thicker fibrous capsules frequently observed at the base of implants in the present study, especially with the smoother surfaces. However, despite the potential dead space at the implant pedestal and obvious difficulty in promoting soft tissue adhesion in this zone, complete attachment in this area was nonetheless observed with the SLA, TPS, and CB samples. Clinical situations may arise where anatomic limitations preclude placement of the endosseous portion of the dental implant in line with the crown. The transmucosal abutment, therefore, must be angulated to reconcile the directional difference between the implant and prosthetic tooth. Such a compromise creates a dead space between the transmucosal abutment and the endosseous implant surface, similar to that encountered in the present experimental design. The roughened surface texture could facilitate soft tissue

adhesion to an angled abutment despite its atypical and unfavorable geometric configuration.

Although statistically significant results were obtained, a limitation of the present study is the relatively small number of PO and FB samples. Many of the retrieved PO surfaces contained extremely supple tissue that did not provide optimal histologic sections. It is possible that extensive fibrous encapsulation around these implants prevented proper resin infiltration during processing. Another problem was that the tissue around many FB and PO samples became detached from the implant surface immediately upon sectioning, rendering them unsuitable for morphometric analysis. These problems limited the numbers of the PO and FB surfaces, but they also provided further evidence that such smooth surfaces are less amenable to a stable connective tissue attachment.

This study was carried out in a subcutaneous rat model. A real challenge exists when rough surfaces penetrate the epithelium and are exposed to the contaminated outside environment, a situation encountered by dental implants and percutaneous devices. The validity of the current findings should be tested in the presence of compounding factors such as oral and skin bacterial flora in the region of the epithelial seal. It would be of interest to conduct subsequent quantitative and qualitative research on connective tissue attachment to transmucosal or percutaneous implants so that the role of rough surface topography on epithelial seal formation could be evaluated.

## CONCLUSIONS

The results indicate that rough implant surfaces are associated with stable connective tissue attachment. In addition, the data from the AE surface may indicate that the geometry of the surface irregularities can also be a significant determinant of the connective tissue response.

## ACKNOWLEDGMENTS

The authors gratefully acknowledge Dr Doug Hamilton for his critical reading of the manuscript, Mr Andre Wong for his technical assistance, and Ms Mabel Cho for designing Fig 2. The original titanium surfaces were provided by the ITI Foundation. This study was supported by the Canadian Institutes of Health Research grant no. 53079.

## REFERENCES

- Brånemark P-I, Adell R, Breine U, Hansson BO, Lindström J, Ohlsson A. Intra-osseous anchorage of dental prostheses. I. Experimental studies. *Scand J Plast Reconstr Surg* 1969;3:81–100.
- Deporter DA, Watson PA, Pilliar RM, Howley TP, Winslow J. A histological evaluation of a functional endosseous, porous-surfaced, titanium alloy dental implant system in the dog. *J Dent Res* 1988;67:1190–1195.
- Buser D, Schenk RK, Steinmann S, Fiorellini JP, Fox CH, Stich H. Influence of surface characteristics on bone integration of titanium implants. A histomorphometric study in miniature pigs. *J Biomed Mater Res* 1991;25:889–902.
- Buser D, Nydegger T, Oxland T, et al. Interface shear strength of titanium implants with a sandblasted and acid-etched surface: A biomechanical study in the maxilla of miniature pigs. *J Biomed Mater Res* 1999;45:75–83.
- Schlegel D, Reichart PA, Pfaff U. Experimental bacteremia to demonstrate the barrier function of epithelium and connective tissue surrounding oral endosseous implants. *Int J Oral Surg* 1978;7:569–572.
- Chehroudi B, Gould TRL, Brunette DM. The role of connective tissue in inhibiting epithelial downgrowth on titanium-coated percutaneous implants. *J Biomed Mater Res* 1992;26:493–515.
- Romeo E, Ghisolfi M, Carmagnola D. Peri-implant diseases. A systematic review of the literature. *Minerva Stomatol* 2004;53:215–230.
- Esposito M, Thomsen P, Ericson LE, Lekholm U. Histopathologic observations on early oral implant failures. *Int J Oral Maxillofac Implants* 1999;14:798–810.
- Esposito M, Thomsen P, Ericson LE, Sennerby L, Lekholm U. Histopathologic observations on late oral implant failures. *Clin Implant Dent Relat Res* 2000;2:18–32.
- Glauser R, Schupbach P, Gottlow J, Hämmerle C. Periimplant soft tissue barrier at experimental one-piece mini-implants with different surface topography in humans: A light-microscopic overview and histometric analysis. *Clin Implant Dent Relat Res* 2005;7(suppl 1):S44–S51.
- von Recum AF, Park JB. Permanent percutaneous devices. *Crit Rev Bioeng* 1981;5(1):37–77.
- von Recum AF. Applications and failure modes of percutaneous devices: A review. *J Biomed Mater Res* 1984;18:323–336.
- Stahl SS. Healing following simulated fiber retention procedures in rats. *J Periodontol* 1977;48:67–73.
- Säuerblich S, Klee D, Richter E-J, Höcker H, Spiekermann H. Cell culture tests for assessing the tolerance of soft tissue to variously modified titanium surfaces. *Clin Oral Implants Res* 1999;10:379–393.
- Holgers KM, Esposito M, Kalltorp M, Thomsen P. Titanium in soft tissues. In: Brunette DM, Tengvall P, Textor M, Thomsen P (eds). *Titanium in Medicine*. Berlin: Springer-Verlag, 2001:514–560.
- Abrahamsson I, Zitzmann NU, Berghlundh T, Linder E, Wennerberg A, Lindhe J. The mucosal attachment to titanium implants with different surface characteristics: An experimental study in dogs. *J Clin Periodontol* 2002;29:448–455.
- Ungersböck A, Pohler O, Perren SM. Evaluation of the soft tissue interface at titanium implants with different surface treatments: Experimental study on rabbits. *Biomed Mater Eng* 1994;4:317–325.
- Keller JC, Schneider GB, Stanford CM, Kellogg B. Effects of implant microtopography on osteoblast cell attachment. *Implant Dent* 2003;12:175–181.
- Brunette DM. Fibroblasts on micromachined substrata orient hierarchically to grooves of different dimensions. *Exp Cell Res* 1986;164:11–26.
- Inoue T, Cox JE, Pilliar RM, Melcher AH. Effect of the surface geometry of smooth and porous-coated titanium alloy on the orientation of fibroblasts in vitro. *J Biomed Mater Res* 1987;21:107–126.
- Lowenberg BF, Pilliar RM, Aubin JE, Gernie GR, Melcher AH. Migration, attachment, and orientation of human gingival fibroblasts to root slices, naked and porous-surfaced titanium alloy discs and Zircalloy 2 discs in vitro. *J Dent Res* 1987;66:1000–1005.
- Abiko Y, Brunette DM. Immunohistochemical investigation of tracks left by the migration of fibroblasts on titanium surfaces. *Cells Mater* 1993;3:161–168.
- den Braber ET, de Ruijter JE, Ginsel LA, von Recum AF, Jansen JA. Quantitative analysis of fibroblast morphology on microgrooved surfaces with various groove and ridge dimensions. *Biomaterials* 1996;17:2037–2044.
- Walboomers XF, Croes HJE, Ginsel LA, Jansen JA. Contact guidance of rat fibroblasts on various implant materials. *J Biomed Mater Res* 1999;47:204–212.
- Schroeder A, van der Zypen E, Stich H, Sutter F. The reactions of bone, connective tissue, and epithelium to endosteal implants with titanium-sprayed surfaces. *J Maxillofac Surg* 1981;9:15–25.
- Jansen JA, Paquay YG, van der Waerden JP. Tissue reaction to soft-tissue anchored percutaneous implants in rabbits. *J Biomed Mater Res* 1994;28:1047–1054.
- Rosengren A, Danielsen N, Persson H, Kober M, Bjursten LM. Tissue reactions to polyethylene implants with different surface topography. *J Mater Sci Mater Med* 1999;10:75–82.
- Lausmaa J. Mechanical, thermal, chemical and electrochemical surface treatment of titanium. In: Brunette DM, Tengvall P, Textor M, Thomsen P (eds). *Titanium in Medicine*. Berlin: Springer-Verlag, 2001:231–266.
- Camporese DS, Lester TP, Pulfrey DL. A fine-line silicon shadow mask for inversion layer solar cells. *IEEE Electron Device Lett* 1981;3:61–63.
- Jaeger N, Brunette DM. Production of microfabricated surfaces and their effects on cell behavior. In: Brunette DM, Tengvall P, Textor M, Thomsen P (eds). *Titanium in Medicine*. Berlin: Springer-Verlag, 2001:348–352.
- Wieland M, Chehroudi B, Textor M, Brunette DM. Use of Ti-coated replicas to investigate the effects on fibroblast shape of surfaces with varying roughness and constant chemical composition. *J Biomed Mater Res* 2002;60:434–444.
- Wieland M, Textor M, Spencer ND, Brunette DM. Wavelength-dependent roughness: A quantitative approach to characterizing the topography of rough titanium surfaces. *Int J Oral Maxillofac Implants* 2001;16:163–181.
- Aebi U, Pollard TP. A glow discharge unit to render electron microscope grids and other surfaces hydrophilic. *J Electron Microscop Tech* 1987;7:29–33.
- Chehroudi B, Gould TRL, Brunette DM. Effects of a grooved epoxy substratum on epithelial cell behavior in vitro and in vivo. *J Biomed Mater Res* 1988;22:459–473.
- Chehroudi B, Brunette DM. Subcutaneous microfabricated surfaces inhibit epithelial recession and promote long-term survival of percutaneous implants. *Biomaterials* 2002;23:229–237.
- Rostlund T, Thomsen P, Bjursten LM, Ericson LE. Differences in tissue response to nitrogen-ion implanted titanium and cp titanium in the abdominal wall of the rat. *J Biomed Mater Res* 1990;24:847–860.

37. Johansson CB, Albrektsson T, Ericson LE, Thomsen P. A quantitative comparison of the cell response to commercially pure titanium and Ti-6Al-4V implants in the abdominal wall of rats. *J Mater Sci Mater Med* 1992;3:126–136.
38. Mohanty M, Hunt JA, Doherty PJ, Annis D, Williams DF. Evaluation of soft tissue response to a poly(urethane urea). *Biomaterials* 1992;13:651–656.
39. Picha GJ, Drake RF. Pillared-surface microstructure and soft-tissue implants: Effect of implant site and fixation. *J Biomed Mater Res* 1996;30:305–312.
40. Cochran DL, Nummikoski PV, Higginbottom FL, Hermann JS, Makins SR, Buser D. Evaluation of an endosseous titanium implant with a sandblasted and acid etched surface surface in a canine mandible: Radiographic results. *Clin Oral Implants Res* 1996;7:240–252.
41. Wennerberg A, Albrektsson T, Andersson B, Krol JJ. A histomorphometric and removal torque study of screw-shaped titanium implants with three different surface topographies. *Clin Oral Implants Res* 1995;6:24–30.
42. Wennerberg A, Albrektsson T, Andersson B. Bone tissue response to commercially pure titanium implants blasted with fine and coarse particles of aluminum oxide. *Int J Oral Maxillofac Implants* 1996;11:38–45.
43. Wennerberg A, Ektessabi A, Albrektsson T, Johansson C, Andersson B. A 1-year follow-up of implants of differing surface roughness placed in rabbit bone. *Int J Oral Maxillofac Implants* 1997;12:486–494.
44. Buser D, Nydegger T, Hirt HP, Cochran DL, Nolte LP. Removal torque values of titanium implants in the maxilla of miniature pigs. *Int J Oral Maxillofac Implants* 1998;13:611–619.
45. Smahel J, Hurwitz PJ, Hurwitz N. Soft tissue response to textured silicone implants in an animal experiment. *Plast Reconstr Surg* 1993;92:474–479.
46. Tarpila E, Ghassemifar R, Fagrell D, Berggren A. Capsular contracture with textured versus smooth saline-filled implants for breast augmentation: A prospective clinical study. *Plast Reconstr Surg* 1997;99:1934–1939.
47. Morehead JM, Holt GR. Soft-tissue response to synthetic biomaterials. *Otolaryng Clin North Am* 1994;27:195–201.
48. Chou L, Firth JD, Uitto VJ, Brunette DM. Substratum surface topography alters cell shape and regulates fibronectin mRNA, mRNA stability, secretion and assembly in human fibroblasts. *J Cell Sci* 1995;108:1563–1573.
49. Hakelius L, Ohlsen L. A clinical comparison of the tendency to capsular contracture between smooth and textured gel-filled silicone mammary implants. *Plast Reconstr Surg* 1992;90:247–254.
50. Batra M, Bernard S, Picha G. Histologic comparison of breast implant shells with smooth, foam, and pillar microstructuring in a rat model from 1 day to 6 months. *Plast Reconstr Surg* 1995;95:354–363.
51. Hakelius L, Ohlsen L. Tendency to capsular contracture around smooth and textured gel-filled silicone mammary implants: A 5-year follow-up. *Plast Reconstr Surg* 1997;100:1566–1569.
52. Wyatt LE, Sinow JD, Wollman JS, Sami DA, Miller TA. The influence of time on human breast capsule histology: Smooth and textured silicone-surfaced implants. *Plast Reconstr Surg* 1998;102:1922–1931.
53. Rubino C, Mazzarello V, Farace F, et al. Ultrastructural anatomy of contracted capsules around textured implants in augmented breasts. *Ann Plast Surg* 2001;46:95–102.
54. Baker JL, Chandler ML, LeVier RR. Occurrence and activity of myofibroblasts in human capsular tissue surrounding mammary implants. *Plast Reconstr Surg* 1981;68:905–914.
55. Lossing C, Hansson H-A. Peptide growth factors and myofibroblasts in capsules around human breast implants. *Plast Reconstr Surg* 1993;91:1277–1286.
56. Coleman DJ, Sharpe IL, Naylor CLC, Cross SE. The role of the contractile fibroblast in the capsules around tissue expanders and implants. *Br J Plast Surg* 1993;46:547–556.
57. Quirynen M, Bollen CML, Papaioannou W, van Eldere J, van Steenberghe D. The influence of titanium abutment surface roughness on plaque accumulation and gingivitis: Short-term observations. *Int J Oral Maxillofac Implants* 1996;11:169–178.
58. Sawase T, Wennerberg A, Hallgren C, Albrektsson A, Baba K. Chemical and topographical surface analysis of five different implant abutments. *Clin Oral Implants Res* 2000;11:44–50.
59. Zitzmann NU, Abrahamsson I, Berglundh T, Lindhe J. Soft tissue reactions to plaque formation at implant abutments with different surface topography. An experimental study in dogs. *J Clin Periodontol* 2002;29:456–461.
60. Wennerberg A, Sennerby L, Kultje C, Lekholm U. Some soft tissue characteristics at implant abutments with different surface topography. A study in humans. *J Clin Periodontol* 2003;30:88–94.
61. Cochran DL, Simpson J, Weber HP, Buser D. Attachment and growth of periodontal cells on smooth and rough titanium. *Int J Oral Maxillofac Implants* 1994;9:289–297.
62. Baharloo B, Textor M, Brunette DM. Substratum roughness alters the growth, area and focal adhesions of epithelial cells, and their proximity to titanium surfaces. *J Biomed Mater Res A* 2005;74(1):12–22.
63. Quirynen M, van der Mei HC, Bollen CML, et al. An in vivo study on the influence of the surface roughness of implants on the microbiology of supra- and subgingival plaque. *J Dent Res* 1993;72:1304–1309.
64. Sanders JE, Rochefort JR. Fibrous encapsulation of single polymer microfibers depends on their vertical dimension in subcutaneous tissue. *J Biomed Mater Res* 2003;67A:1181–1187.